# The isthmic neuroepithelium is essential for cerebellar midline fusion

**Angeliki Louvi[1,*], Paula Alexandre[1], Christine Métin[1,†], Wolfgang Wurst[2] and Marion Wassef[1,‡]**

[1]Régionalisation Nerveuse CNRS/ENS UMR 8542, Ecole normale supérieure, 46 rue d'Ulm, 75005 Paris, France
[2]GSF-Research Centre, Institute of Mammalian Genetics, Ingolsträdter Landstrasse 1, D-85764 Neuherberg and Max-Planck-Institute of Psychiatry, Kraepelinstrasse 2-10, D-80809 Munich, Germany
*Present address: Department of Neurobiology, Pharmacology and Physiology, University of Chicago, Chicago, IL 60637, USA
†Present address: INSERM U106, Hôpital de la Salpêtrière, 47 bd de l'Hôpital, 75013 Paris, France
‡Author for correspondence (e-mail: wassef@wotan.ens.fr)
This paper is dedicated to Cuca Alvarado-Mallart who retired recently

*Accepted 21 July 2003*

Development 130, 5319-5330

doi:10.1242/dev.00736

## Summary

**The cerebellum comprises a medial domain, called the vermis, flanked by two lateral subdivisions, the cerebellar hemispheres. Normal development of the vermis involves fusion of two lateral primordia on the dorsal midline. We investigated how the cerebellum fuses on the midline by combining a study of mid/hindbrain cell movements in avian embryos with the analysis of cerebellar fusion in normal and mutant mouse embryos. We found that, in avian embryos, divergent cell movements originating from a restricted medial domain located at the mid/hindbrain boundary produce the roof plate of the mid/hindbrain domain. Cells migrating anteriorly from this region populate the caudal midbrain roof plate whereas cells migrating posteriorly populate the cerebellar roof plate. In addition, the adjacent paramedial isthmic neuroepithelium also migrates caudalward and participates in the formation of the cerebellar midline region. We also found that the paramedial isthmic territory produces two distinct structures. First, the late developing velum medullaris that intervenes between the vermis and the midbrain, and second, a midline domain upon which the cerebellum fuses. Elimination or overgrowth of this isthmic domain in *Wnt1*$^{sw/sw}$ and *En1*$^{+/Otx2lacZ}$ mutant mice, respectively, impair cerebellar midline fusion. Because the isthmus-derived midline cerebellar domain displays a distinct expression pattern of genes involved in BMP signaling, we propose that the isthmus-derived cells provide both a substratum and signals that are essential for cerebellar fusion.**

Key words: Cerebellum, Cerebellar midline fusion, Roof plate, Mid/hindbrain morphogenesis, Isthmus, Velum medullaris, Choroid plexus, Wnt1, Engrailed, Otx2, Swaying, Chick-quail chimera, Mouse

## Introduction

The adult cerebellar cortex is subdivided mediolaterally into biochemically distinct functional subdomains organized into sagittal stripes or patches that may be considered as functional equivalents of the cortical areas of the mammalian cerebral cortex (Andersson and Oscarsson, 1978; Hawkes and Eisenmann, 1997). Histological (Altman and Bayer, 1985a; Altman and Bayer, 1985b), transplantation (Alvarez Otero et al., 1993; Hallonet et al., 1990; Hallonet and Le Douarin, 1993; Martinez and Alvarado-Mallart, 1989) and cell lineage (Lin and Cepko, 1999; Mathis et al., 1997) tracing studies have indicated that, in the course of embryonic development, the cerebellar primordium rotates in such a way that its anteroposterior axis becomes mediolateral. The rotation seems to result from early cell rearrangements at the mid/hindbrain (MHB) junction (Millet et al., 1996) and involves a territory fated to produce isthmic structures and the vermis region of the cerebellum (Hallonet et al., 1990; Martinez and Alvarado-Mallart, 1989). Several observations indicate that Purkinje cells or deep nuclei neurons deriving from a single progenitor do not cross the midline (Alvarez Otero et al., 1993; Hallonet and Le Douarin, 1993; Herrup et al., 1984; Herrup and Kuemerle, 1997; Lin and Cepko, 1999; Mathis et al., 1997). This suggests that the cerebellar vermis develops from a pair of separate primordia. Mutations affecting the MHB organizer result in deletion of the vermis and part of the cerebellar hemispheres (Broccoli et al., 1999; Favor et al., 1996; Liu and Joyner, 2001; McMahon and Bradley, 1990; Thomas and Cappechi, 1990; Thomas et al., 1991; Shimamura et al., 1994; Wurst et al., 1994). While these mutations do not affect neural tube closure, the cerebellar remnants do not fuse on the midline, but stay widely separated, suggesting that morphogenetic movements or specific isthmic or vermal structures are required for cerebellar fusion.

In the present study we explored how and when midline fusion of the cerebellum takes place. To gain insight into this process, we first produced a new fate map of the MHB in avian embryos by following the fate of calibrated circular grafts and by labeling small groups of cells with DiI. The fate map revealed marked variations in growth between the medial and lateral domains of the caudal midbrain neuroepithelium that could influence morphogenetic movements. In addition, at stage 10-11 according to Hamburger and Hamilton (HH10-11) (Hamburger and Hamilton, 1951), we detected two distinct

domains that contributed cells to the cerebellar midline: a restricted isthmic midline domain produced divergent flows of cells that populated the roof plates of the caudal midbrain and anterior hindbrain, and an adjacent domain contributed to the velum medullaris, a structure that links the cerebellar vermis to the inferior colliculus, and also provided a substratum for midline cerebellar fusion. This domain was considered distinct from the vermis primordium because it produced none of the typical cerebellar cell types (granule cells, Purkinje, Golgi or deep cerebellar nuclei neurons).

We then turned our attention to the mouse, in which not only have many regional and cell-type specific markers of the early and late cerebellum been characterized, but also a large number of cerebellar mutants is available. Examination of cerebellar fusion in wild-type mice suggested that BMP signaling was transiently decreased at the cerebellar midline. In addition, just before the onset of granule cell progenitor (GCP) production at early E14.5, expression of the rhombic lip marker Math1 (Atoh1) was downregulated at the medial roof plate segment separating the two vermis primordia, thus allowing for midline cerebellar fusion. Together, these observations indicated that the isthmus-derived cerebellar midline cells have distinct signaling properties.

Based on the avian fate map and on observations in wild-type mice and in *Wnt1*$^{sw/sw}$ [*swaying* (Lane, 1967; Bronson and Higgins, 1991; Thomas et al., 1991)] and *En1*$^{+/Otx2lacZ}$ mutant embryos (Broccoli et al., 1999), and in *En1*$^{hd/hd}$ adult survivors (Wurst et al., 1994), we propose that the caudalward movement of isthmus-derived cells is essential for cerebellar fusion for two reasons. First, because it provides a favorable cell substratum; second, because its distinct signaling properties modify the edges of the two cerebellar primordia at the midline rhombic lip allowing for fusion to occur and possibly restricting the rostral extension of the presumptive choroid plexus territory that depends on BMP signaling.

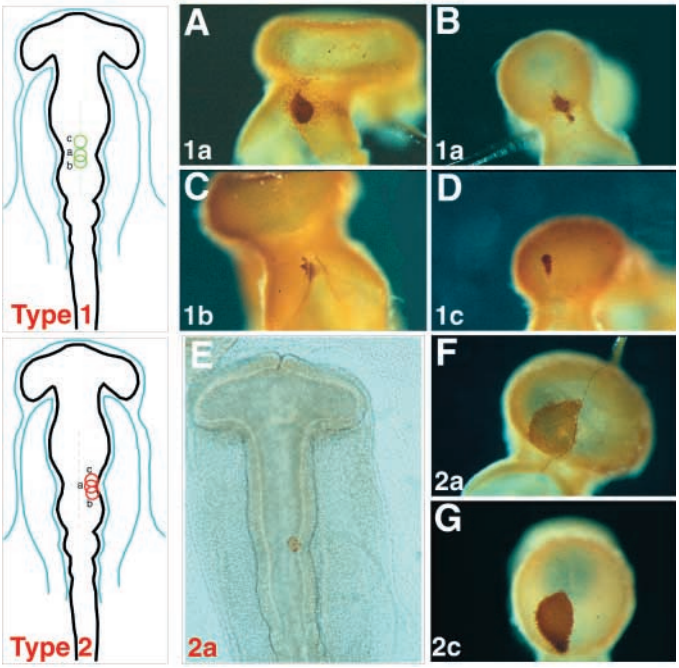


**Fig. 1.** Transplantation experiments. In this and the next figure, schematic representations of isotopic and isochronic graft types are shown on the left, and the grafted quail cells (in brown) are visualized by anti-QCPN immunohistochemistry. (A-D) Dorsomedial (type 1) grafts. (A,B) Grafts centered on the isthmus (type 1a) move caudally and are detected in the hindbrain (A; 78% of the cases) or straddling the MHB (mid/hindbrain) (B; 11%). (C,D) When grafts are placed caudal (type 1b; C) or rostral (type 1c; D) to the isthmus, they are detected, respectively, in the hindbrain or the midbrain. (E-G) Lateral (type 2) grafts. (E) Example of an embryo with a type 2a graft, fixed 2 hours post-transplantation. (F) Grafts positioned laterally (example of a graft to the left side) at the level of the isthmus (type 2a) move rostromedially and are detected significantly enlarged in the midbrain. (G) Grafts positioned just rostral to the isthmus (type 2c) move rostromedially.

## Materials and methods

### Chick embryos

White Leghorn chick embryos (Morizeau, France) and Japanese quail embryos (La Caille de Chanteloup, France) were staged according to Hamburger and Hamilton (Hamburger and Hamilton, 1951).

### Mouse strains

Wild-type embryos were of the OF1 strain (IFFA Credo, France) or littermates of the mutant embryos. Mutant strains were described previously: (i) *Wnt1*$^{sw/sw}$ (Lane, 1967; Thomas et al., 1991) (purchased from the Jackson Labs); (ii) *En1*$^{+/Otx2lacZ}$ [*Otx2 lacZ* knock-in into the *En1* locus (Broccoli et al., 1999)]; (iii) *En1*$^{hd}$ [hd: homeodomain deletion (Wurst et al., 1994)]; (iv) *En1*$^{Lki}$ [Lki: *lacZ* knock-in into the *En1* locus (Hanks et al., 1995)]. Genotyping of *Wnt1*$^{sw/sw}$ embryos was as described previously (Bally-Cuif et al., 1995). Adult cerebella were fixed in 4% paraformaldehyde and stained in toto with India ink to reveal foliation details.

### Transplantation experiments

The different types of homotopic and isochronic transplantation experiments between quail donor and chick host embryos are schematically represented in Figs 1 and 2 (left). For microsurgery, we used hand-made microscalpels and drawn-out glass micropipettes (Clark Electromedical Instruments, cat. no. GC100T-15), with tips of known diameter (50 or 100 μm), measured with a micrometer under a dissecting microscope. Briefly, host chick embryos at the 9- to 13-somite stage (ss) (HH9-11) were visualized by a sub-blastodermal injection of India ink. Through a cut in the vitelline membrane, a small plug (100 μm in type 1-3 and 50 μm in type 5 grafts) or a thin strip (type 4 grafts) was removed from the dorsal neuroepithelium. The corresponding size-matched portion of neuroepithelium was isolated from a donor quail embryo using the same micropipette without enzymatic dissociation and transported to replace the ablated region on the chick host. The eggshell was sealed with tape and returned to the incubator. Most embryos were collected at HH19-21 (E4) and fixed by immersion in sodium phosphate buffered 4% paraformaldehyde prior to immunohistochemistry. Type 4 chimeras (see below) that were allowed to survive until E16, E18 or E19 were fixed by transcardiac perfusion of the same fixative.

#### Type 1: dorsomedial grafts (Fig. 1, left; upper panel)

Circular grafts including the dorsal midline, were subdivided into three groups, depending on their positioning along the rostrocaudal axis. Type 1a grafts were centered on the isthmus; semi-circular grafts, with a medial limit at the dorsal midline were also included in this group. Type 1b grafts were placed just caudal to the isthmus, and type 1c grafts rostral to it.

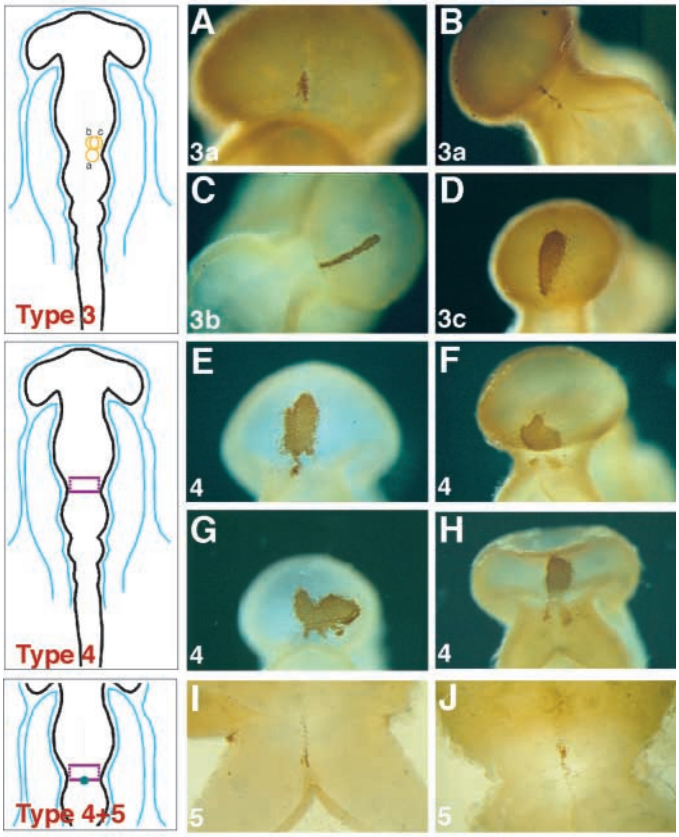


**Fig. 2.** Transplantation experiments. (A-D) Paramedial (type 3) grafts. (A-C) Grafts placed close to the midline (type 3a and 3b) are found elongated bordering on the midline. When placed at the isthmus (type 3a), they end up either in the midbrain (A) or straddling the MHB (B), while when placed rostral to the isthmus (type 3b), they become elongated in the caudal midbrain (C). (D) Grafts placed rostral to the isthmus and at a distance from the midline (type 3c) move rostromedially in the midbrain but are no longer elongated and have increased in size relatively to the grafts placed closer to the midline. (E-H) Bilateral dorsal strip (type 4) grafts of the caudal midbrain move rostromedially but also caudally in the hindbrain where they contribute to thin medial streams of cells that avoid the roof plate. (I,J) Small midline (type 5) grafts. Small grafts centered on the isthmus contribute modestly to the midline either exclusively in the hindbrain (I; flat-mount view of the grafted embryo) or straddling the MHB (J; ibid.).

Type 2: lateral grafts (Fig. 1, left; lower panel)

Circular lateral grafts (mostly on the right side of the embryo, but some were placed on the left) that excluded the dorsal midline, subdivided into three overlapping groups. Type 2a grafts were centered on the isthmus. Type 2b grafts were placed caudal to the isthmus, with their rostral end positioned at the level of the constriction. Type 2c grafts were placed rostral to the isthmus, with their caudal end positioned at the level of the constriction.

Type 3: paramedial grafts (Fig. 2, left; upper panel)

Circular grafts, intermediate in position between type 1 and type 2 grafts, extending medially to the dorsal midline (which they barely touched). Type 3a grafts were centered on the isthmus. Type 3b and 3c grafts partially overlapped and were placed rostral to the isthmus, the former close to the midline and the latter slightly more laterally.

Type 4: strip grafts (Fig. 2, left; middle panel)

Bilateral stripped grafts positioned at the caudal end of the midbrain.

Type 5: midline grafts (Fig. 2, left; lower panel)

Small sized grafts (about 50 μm), encompassing the dorsal midline at the isthmus.

### Immunohistochemistry

Embryos were fixed by immersion in 4% paraformaldehyde overnight at 4°C and the neural tubes were dissected free of surrounding mesenchyme, dehydrated in methanol and then rehydrated prior to incubation in 0.1% $H_2O_2$ in PGT (PBS, 0.2% gelatin, 1% Triton X-100). Immunohistochemistry on embryos or cryosections was performed as described previously (Louvi and Wassef, 2000). Nissl staining was performed by standard procedures.

The QCPN (DSHB, diluted 1:10), anti-BrdU (Becton Dickinson, diluted 1:400), anti-calbindin $D_{28K}$ (Swant; diluted 1:10000), anti-parvalbumin (Sigma; diluted 1:10000), anti-QH1 (a gift from A. Eichmann; diluted 1:5) and anti-vimentin (Amersham; diluted 1:5) monoclonal antibodies, and a rabbit anti-GFAP (Dako, diluted 1:1000) were used to detect quail cells, BrdU, Purkinje cells, interneurons, quail-derived vessels, radial glia and astrocytes, respectively.

### Analysis of cell movements

Following immunostaining, camera lucida drawings of individual embryos with integrated grafts were produced. The embryos were photographed as whole mounts. Embryos within each graft subtype were divided into four age groups, based on the number of somites (s; 8/9s, 10s, 11s and 12/13s) and movements of quail cells with respect to the initial position of the graft were recorded. Cell movements were consistent across all four age groups, and the presented results are compilations.

### DiI labeling in chick embryos and in *En1*$^{+/Otx2lacZ}$ mouse mutants

Fertilized eggs were incubated to the 10ss (somite stage) and windowed. A small area of the vitelline membrane was removed over the MHB, and a solution of DiI (Molecular Probes Inc.) at 5 mg/ml in dimethylformamide was injected onto the dorsal neural tube, from a pulled glass pipette. Embryos were either fixed 1 hour after DiI application in 4% paraformaldehyde at 4°C, or allowed to proceed to stages HH19-21, then fixed. Embryos at HH10 were photographed as whole mounts in fluorescent and polarized light and the two images were superimposed using Adobe PhotoShop. Embryos at HH19-21 were dissected and the MHB region was flat-mounted. Pictures were taken using a Zeiss Axioscope microscope.

Small DiI crystals were inserted into the axonal bundle that links the two hemicerebella in paraformaldehyde fixed *En1*$^{+/Otx2lacZ}$ mutants at postnatal day (P) 4.

### BrdU labeling

Pregnant females were injected intraperitoneally with a solution of BrdU (2 mg/ml in saline) at 20 μg/g of body weight and sacrificed 2 hours later. Proliferating granule cell precursors at the surface of the cerebellar anlage were revealed by whole-mount immunohistochemistry.

### In situ hybridization

Fixed embryos were hybridized in toto with one or two riboprobes as described previously (Bally-Cuif et al., 1995), with minor modifications for cryostat, frozen or vibratome sections of E16-E20 embryos. Probes used were: Math1 (a gift from F. Guillemot); Roro α (a gift from B. Hamilton), Ttr (a gift from W. Blaner); Slit2 (a gift from A. Chédotal and M. Tessier-Lavigne); chick Gdf7 (a gift from K. Lee); mouse Wnt1 (a gift from J. Kitajewski); Drm (a gift from M.

Marx); rat Gad67 (a gift from A. Tobin); chick GAD67 (a gift from C. Ragsdale).

## Results

### Calibrated homotopic grafts reveal local differences in growth in the developing midbrain

To trace cell movements at the MHB, we took advantage of the chick-quail transplantation system (Le Douarin, 1969). First, a series of homotopic and isochronic circular grafts of known diameter (100 μm) were performed at HH10 and analyzed 2 days later at HH19-21, when the isthmic constriction coincides with the limit between the midbrain and anterior hindbrain (Hallonet et al., 1990; Martinez and Alvarado-Mallart, 1989; Millet et al., 1996). Use of calibrated grafts ensured accelerated healing, reduced variability, and allowed for comparison of growth rates. Although the quail cells remained clustered in the host embryo, the grafts were no longer circular, revealing morphogenetic movements. The size of the graft-derived area at E4 depended upon the anteroposterior and mediolateral coordinates of the graft at E2. Medial grafts encompassing (but not restricted to) the dorsal midline increased in size only modestly. In contrast, the greater its distance from the midline, the larger a graft became (compare for example grafts 1c with 2c in Fig. 1, and 3b with 3c in Fig. 2). These differences cannot be attributed to differential cell death, since no remarkable patterns of necrotic cells were evident in the dorsal midbrain in normal embryos between stages HH10 and 23, with the exception of the dorsal midline (Alexandre and Wassef, 2003; Lumsden et al., 1991; Lawson et al., 1999).

Therefore, distinct regions of the developing dorsal midbrain are characterized by differential growth.

### Analysis of cell movements in the dorsal mid/hindbrain

#### I. Dorsomedial (type 1) grafts

To follow the movements of dorsomedially located cells, we analyzed embryos with grafts encompassing the midline at different rostrocaudal levels (Fig. 1A-D). Type 1a grafts (*n*=27), placed at the isthmus, were mainly (21/27) found in the hindbrain at HH19-21 (Fig. 1A). A few (3/27) were found elongated and straddling the MHB (Fig. 1B), while another few (3/27) ended up anterior to the MHB and were confined to the midbrain. Type 1b grafts (*n*=2) remained in the hindbrain (Fig. 1C), while type 1c grafts (*n*=7) were almost invariably (6/7) restricted to the midbrain (Fig. 1D), with the exception of one graft which extended thinly into the hindbrain (not shown).

#### II. Lateral (type 2) grafts

To address whether cells located laterally in the alar plate undergo movements similar to those observed medially, we analyzed embryos with dorsolateral grafts (Fig. 1E-G). Type 2a (Fig. 1E) and 2b grafts behaved similarly (*n*=5+2). Some (3/7) were displaced rostromedially close to the midbrain midline at HH19-21 and had increased in size (Fig. 1F); others (2/7) extended on both sides of the MHB, medially into the midbrain and laterally into the hindbrain, yet others (2/7), moved caudolaterally and were confined to the hindbrain (not shown). Type 2c grafts (*n*=8) moved rostromedially (5/8), close to (but respecting) the midline of the midbrain and were significantly enlarged as well (Fig. 1G), or extended on both sides of the MHB (3/8), with their rostral part elongated rostromedially and the caudal part having moved caudolaterally into the hindbrain (not shown).

#### III. Paramedial (type 3) grafts

To examine cell movements adjacent to the dorsal midline, we analyzed embryos with grafts placed between the midline and the lateral edge of the dorsal midbrain at different rostrocaudal positions (Fig. 2A-D). Type 3a isthmic grafts (*n*=3), became elongated very close to the midline, and moved along the anterior-posterior axis, either rostrally (Fig. 2A), or caudally, or even in both directions, split in half (Fig. 2B). Type 3b grafts (*n*=7) retained their medial position. They, too, became elongated close to the dorsal midline, but were larger in comparison with type 3a grafts (Fig. 2C). Type 3c grafts (*n*=8) moved rostromedially (7/8) towards the midline and, compared to type 3a and 3b grafts, increased significantly in size (Fig. 2D).

#### IV. Strip (type 4) and midline (type 5) grafts

In order to directly assess the convergent movements of the neuroepithelium, revealed by type 1-3 grafts, we performed thin bilateral strip grafts that encompassed the entire dorsal part of the caudal midbrain (Fig. 2E-H). In agreement with our previous observations, descendants of these strip grafts (*n*=17) were confined to the medial-most MHB structures (13/17); in the hindbrain they formed two bilateral and distinct protrusions (see for example Fig. 2F,H). In the remaining cases (4/17), QCPN-positive cells were exclusively encountered in the midbrain, rostral to the MHB. Analysis of long survival strip grafts (*n*=4) at E16 allowed us to assess their contribution to hindbrain structures (see below).

Finally, we performed a series of small grafts at the level of the isthmus, as restricted to the dorsal midline as possible (Fig. 2I,J). These grafts became extremely thin and elongated, and remained strictly confined within the midline. Consistently, only a few quail cells were detected 2 days after grafting, in the majority of cases (11/19) along the midline of the cerebellar plate, in agreement with the results obtained with type 1 grafts (Fig. 2I). Extensive cell death affecting the MHB midline region at the 14-16ss (Lumsden et al., 1991) and, possibly, a lower proliferation rate could explain why the small transplants only contributed scattered cells to the cerebellar midline. In some embryos (4/19), quail cells were detected rostrally within the midline of the caudal midbrain, while in the remaining cases (4/19), they were present on both sides of the MHB, yet were always confined to the midline (Fig. 2J).

### Tracing the cells at the MHB with DiI

To corroborate the results of our grafting experiments we labeled cells located at and rostral to the isthmus with DiI at the 10ss, and monitored their distribution 2 days later. Observation of embryos fixed 1 hour after DiI application, confirmed that only a small cluster of cells at the desired position was labeled (Fig. 3A-D). When DiI was applied dorsomedially at the level of the constriction (Fig. 3A,B), labeled cells were found either exclusively along the midline of the cerebellar plate (Fig. 3E), or in the midline of the caudal midbrain as well (Fig. 3F), reflecting the movements of type 1a and 5 grafts. Midline cells located rostral to the constriction at the time of DiI application (Fig. 3C), were encountered in

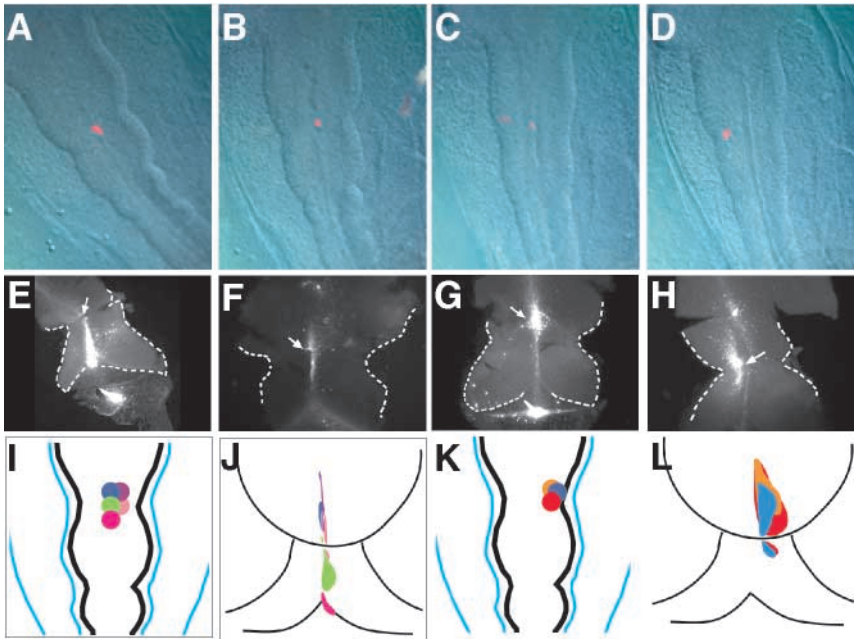


**Fig. 3.** (A-H) DiI labeling of cells at the isthmus. (A-D) Examples of embryos labeled with DiI at the 10ss and fixed 1 hour after labeling. (A) Dorsomedial, (B) small midline, (C) rostral to constriction, and (D) paramedial DiI application sites. (E,F) Examples of embryos fixed at E4; the MHB region is flat-mounted. Dorsomedially located cells participate in the cerebellar midline (E), or, in addition, to the midline of the caudal midbrain (F). Cells located medially but anterior to the isthmus, are confined to the caudal midbrain (G). Cells at paramedial isthmic locations are found on both sides of the MHB (H). Arrows indicate DiI application sites. (I-L) Cell movements in the isthmus. (I) Summary of medial and paramedial grafts at E2 (HH10). (J) At E4, medially located isthmic cells (in green) have preferentially moved in a caudal direction, while cells rostral (in blue) or caudal (in bright pink) to them, have moved, respectively, to the caudal midbrain or the edge of the cerebellar plate. Paramedially located cells (in purple and pink) move rostromedially towards the midline. (K) Summary of lateral grafts at E2 (HH10). (L) At E4, laterally located isthmic cells (in red) have moved rostromedially or caudomedially. Cells located rostrolaterally to the constriction (in blue and orange), have moved rostromedially. In J and L, compare the relative size of the grafts at E4, which depends on the initial transplantation site.

the caudal midbrain at HH19-21 (Fig. 3G), much as type 1c grafts. Finally, when DiI was applied next to the midline at the constriction (Fig. 3D), labeled cells were found paramedially, in both the caudal midbrain and the rostral hindbrain (Fig. 3H). Thus, the DiI labeling experiments faithfully reproduced the results of the transplantation experiments. Cell movements at the MHB are summarized in Fig. 3I-L.

Collectively, our results demonstrate that the cerebellar roof plate develops from a restricted region at the MHB junction that is distinct from the more lateral vermis primordium. In addition, they point to differences in local growth as a possible influence on morphogenetic cell movements.

### The isthmic interface contributes to the velum medullaris and the anterior cerebellum

Our transplantation and DiI tracing experiments indicated that the dorsal isthmic neuroepithelium contributes to the midline of the cerebellar plate. To assess the differentiation of strip graft-derived cells, we analyzed long-survival type 4 chimeras at E16, E18 and E19. In all cases (4/4) the grafts contributed to the anterior cerebellum and to the velum medullaris, a sheet of cells that links the cerebellar vermis with the midbrain and constitutes the roof of the fourth ventricle in this region (Fig. 4A,B). In agreement with earlier reports (Hallonet et al., 1990; Martinez and Alvarado-Mallart, 1989), the strip grafts contributed neither granule cells (GCs) nor deep nuclei neurons to the cerebellum. The strip grafts contributed only a few large neurons to the Purkinje or granular layers (putative PC and Golgi cells, respectively) (Fig. 4C) and these neurons were even completely absent from 2 out of 4 strip grafts at E16 (Fig. 4D). The distribution of quail cells in the cerebellum of strip graft chimeras (type 4) was distinct: a great number of small quail cells accumulated around the Purkinje cell (PC) somata and in the vicinity of the white matter. This pattern closely resembles that of the small GAD67-positive cells (Fig. 4E). In order to better characterize the cerebellar cell types produced by the strip grafts, several markers were used. Parvalbumin, a marker of PCs and of the interneurons of the molecular layer (MLI) (Alvarez Otero et al., 1993) was not expressed in the MLI at E16; however, a few putative MLI in the molecular layer of E16 control chick embryos expressed GAD67 transcripts (Fig. 4E). Unfortunately, the hybridization procedure prevented the subsequent detection of the two available quail cell markers: the QCPN epitope and the nucleolus-associated chromatin. Comparison of GAD and parvalbumin staining at E18-E20 indicated that only a modest proportion of the GAD-positive MLI expressed parvalbumin (Fig. 4F-H). Accordingly, only a small proportion of the quail MLI expressed parvalbumin in type 4 chimeras at E18 (Fig. 4G). A few vascular segments in the molecular and granular layers expressed the quail endothelium marker QH1 (Fig. 4I), and some GFAP-positive quail-derived astrocytes were detected in axonal tracts (Fig. 4J).

The observation that although some strip grafts populated the cerebellar midline, they produced none of the typical cerebellar cell types, namely PCs, Golgi or GCs, is consistent with the interpretation that the isthmus-derived neuroepithelium that intervenes between the two cerebellar primordia is distinct from them.

### Fusion of the mouse cerebellar cortex

The chick fate map pointed to the contribution of a dorsal isthmic domain to the midline of the cerebellum, providing it with a substratum for fusion. However, limitations of the avian system, notably the lack of genetic tools, led us to analyze cerebellar cortex fusion in the mouse where many cerebellar markers and mutants are available. The two major cell types of the cerebellar cortex, PCs and GCs, have distinct origin: PCs

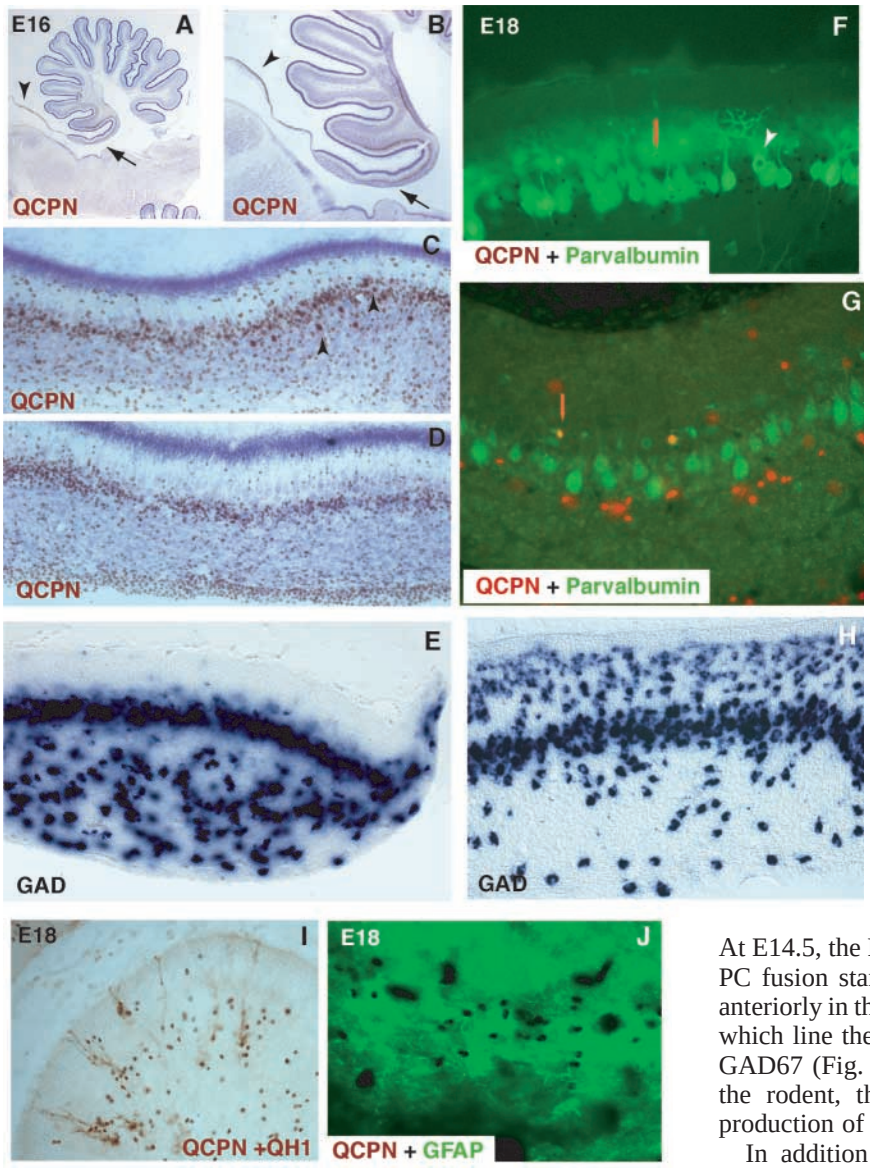


**Fig. 4.** The strip grafts (type 4) contribute to the cerebellar midline but produce none of the main cerebellar cell types. Sagittal sections through the MHB region of E16 (A-D) and E18 (F,G,I,J) chick-quail chimeras that received type 4 transplants. (A,B) The grafts contribute to the velum medullaris (arrowheads) and to the medial cerebellum (arrows). (C,D) Higher magnifications illustrating the graft-derived cell types. None of the grafts produced granule cells or deep nuclear neurons. Half of the grafts produced typical cerebellar cell types i.e. Purkinje and Golgi cells (arrowheads in C and F). The other half produced exclusively glial cells and interneurons of the molecular layer (D) suggesting that they arose from the frontier of the cerebellar anlage. (E,H) The number of molecular layer interneurons that express GAD67 increases significantly between E16 and E18 in the normal chick embryo. (F,G,I,J). The grafts produced only scarce Purkinje cells (F) or molecular layer interneurons (G), both detected by parvalbumin immunohistochemistry, a few QH1-positive vascular elements in the molecular and granular layers (I), and some astrocytes (J).

are produced by the cerebellar neuroepithelium, whereas GCs derive from proliferative precursors (GCPs) generated by the anterior rhombic lip (Alcántara et al., 2000; Gilthorpe et al., 2002; Wingate and Hatten, 1999). We examined cerebellar development using two cell type-specific markers (Fig. 5A): for the rhombic lip and GCPs, Math1, a transcription factor required for the development of rhombic lip derivatives (Ben-Arie et al., 1997; Ben-Arie et al., 2000) and for PCs, Rorα an orphan nuclear receptor (Hamilton et al., 1996).

Between E11.5 and E13.5, the precursors of GCs and PCs develop in discrete territories on each side of the midline. Until E13.5, the Math1-labeled rhombic lip completely outlines the two cerebellar plates up to the MHB junction, intervening in particular between the two adjacent vermis primordia (Fig. 5B). By E14.5, the GCPs, identified by Math1 and BrdU expression, migrate from the caudal rhombic lip and form a continuous layer across the surface of the developing cerebellum (Fig. 5C-E). Meanwhile, Math1 expression decreases in the medial rhombic lip except for a patch that persists at the MHB junction. No longer is there continuity between this expression site and the GCPs (Fig. 5C). Thus, between E13.5 and E14.5 the medial rhombic lip neuroepithelium loses expression of Math1. At E13.5, just after the peak of their production, PCs are detected in two crescent-shaped domains separated medially by a Rorα-negative region (Fig. 5F). At E14.5, the PCs still avoid a wide midline domain (Fig. 5G). PC fusion starts caudally by E15 (Fig. 5H,I) and progresses anteriorly in the following days. Inside the gap, two cell stripes, which line the roof plate on each side, express high levels of GAD67 (Fig. 5J) and GABA (not shown), suggesting that in the rodent, the cerebellar midline is also involved in the production of GABAergic interneurons.

In addition to the loss of Math1 expression at E14.5, a distinct pattern of expression of signaling molecules is observed at the cerebellar midline, in both mouse and chick. For example, expression of BMP/TGFβ-related genes is delayed in the MHB midline: BMP5 and BMP7 in chick (Fig. 5K), Gdf7 in chick (Fig. 5L) and mouse (not shown), whereas between E9.5 and E11.5 in mouse embryos, the cerebellar roof plate is precisely outlined by a transient expression of Drm, a potent BMP antagonist of the Cerberus family (Pearce et al., 1999); (Fig. 5M). This suggests that BMP signaling is transiently down regulated at the MHB junction. Previous studies have also shown that the expression of factors belonging to other families of signaling molecules, such as Slit1/2 in mouse (Yuan et al., 1999) (Fig. 5N) and Wnt1 in both chick and mouse (Bally-Cuif and Wassef, 1994), is also interrupted on the cerebellar roof plate.

## Development of the velum medullaris

In the late mouse embryo the medial cerebellum (delimited rostrally by the extension of the external granular layer; EGL) almost abuts the caudal midbrain boundary (Fig. 6A). The ependymal domain (Fig. 6A, arrow) corresponding to the

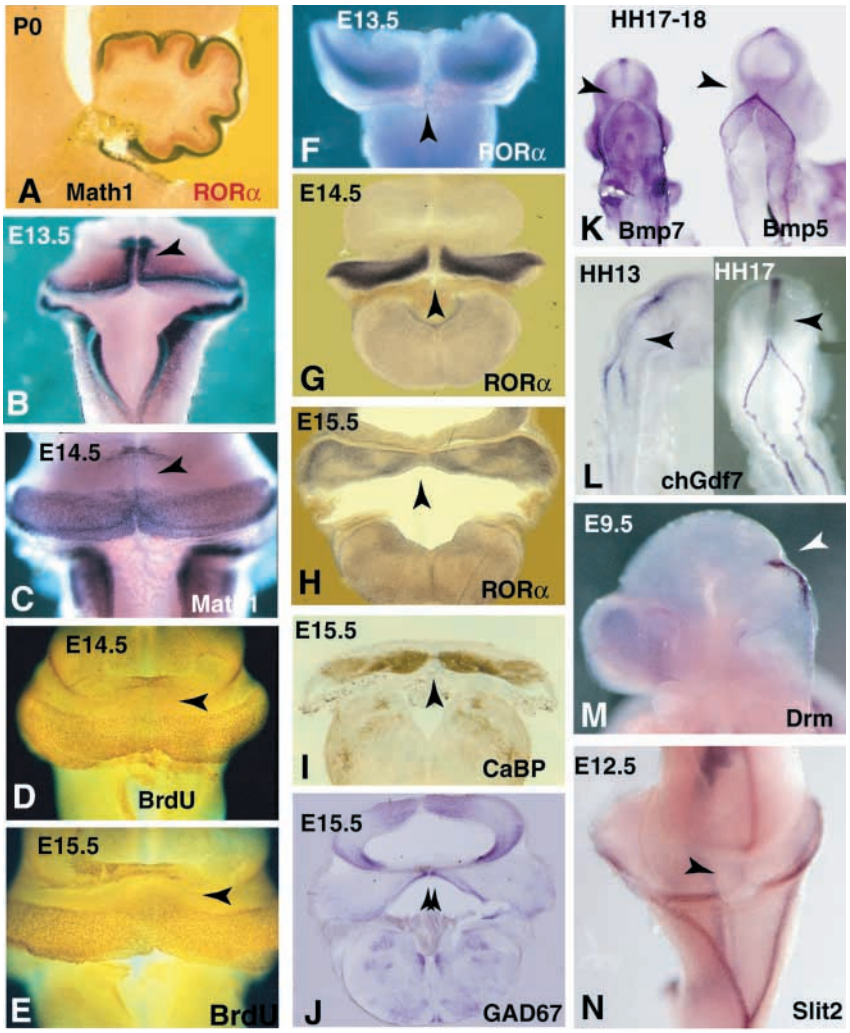


**Fig. 5.** Cerebellar midline fusion and variations in the expression of roof plate markers at the MHB junction. (A) Sagittal section of the cerebellum of a newborn mouse. PCs and GCPs are labeled by in situ hybridization for the detection of Rorα (red) and Math1 (blue) transcripts, respectively. (B,C) Math1 is expressed in the hindbrain rhombic lip including the cerebellar midline (arrowhead in B) until E13.5. Math1 expression is downregulated on the cerebellar midline at E14.5 (arrowhead in C) when the GCPs begin to form the external granular layer. (D,E) The proliferating GCPs, labeled by incorporation of BrdU, extend rostrally between E14.5 and E15.5, in particular in the midline region (arrowheads). (F-I) PCs are detected at successive developmental stages (top left of each picture) in whole-mount cerebellum (F) or transverse vibratome sections (G-I) by Rorα in situ hybridization (F-H) or CaBP (calbindin, I) immunocytochemistry. PCs are at first excluded from the midline region (arrowhead in F,G), which becomes secondarily colonized by E15.5 (arrowhead in H,I). (J) In mouse the cerebellar midline expresses high levels of GAD67 transcripts suggesting its specialization in the production of GABAergic interneurons. (K-N) Expression of dorsal midline markers is distinctly modulated in the MHB region (arrowheads) of chick (K,L) and mouse (M,N) embryos.

isthmus at this stage is narrow. During the next few days, a wide thin sheet of cells devoid of neurons, the velum medullaris, characterized by En1 expression, develops in this region, linking the anterior vermis to the inferior colliculus of the midbrain (Fig. 6B,C). Two processes contribute to the growth of the velum medullaris in the mouse. On the one hand, active proliferation, as the proportion of BrdU-labeled ependymal cells is higher in the velum than in the cerebellum in perinatal rodents (Fig. 6D). On the other hand, we observed a shortening of the midline cerebellar ependyme in P4 pups, in comparison to late gestation embryos (not shown). A posterior retraction of the anterior end of the vermis causes the velum to delaminate form the anterior cerebellum and expand. This process may involve a set of radial glia, labeled by vimentin, which link the anterior and posterior edges of the vermis (Fig. 6E,F) and express high levels of En1 (Fig. 6G). These glia progressively detach from the ependymal surface (Fig. 6G and data not shown). Thus, our observations in avian and rodent embryos indicate that the cerebellum fuses over an isthmic-derived territory, which, in rodent, is subsequently relinquished to the velum medullaris.

A schematic interpretation of the morphogenetic movements that result in cerebellar midline fusion, based on our observations in both chick and mouse, is provided in Fig. 7.

## Development of midline structures in mid/hindbrain mutants

In light of our observations, it is striking that partial loss or gain of function of mouse genes documented to affect MHB development in the mouse often result in defects in cerebellar midline fusion (Broccoli et al., 1999; Bronson and Higgins, 1991; Li et al., 2002). We sought genetic evidence for a role of En1, Wnt1, and Otx2 in the development of midline structures. Having observed that En1 is highly expressed in the velum medullaris (Fig. 5B,C), we analyzed *En1*$^{hd/hd}$ mutant survivors. Although all *En1*$^{hd/hd}$ mutants maintained on inbred 129/Sv or mixed C57Bl/6Jx129/Sv background die at birth with a large deletion of the MHB region (Wurst et al., 1994), a few mutants survive to adulthood on C57Bl/6J background. The cerebellum of these *En1*$^{hd/hd}$ survivors is often fused on the midline despite the reduction in size of the vermis (Fig. 8A,C). On midsagittal sections (Fig. 8B,D), a short velum is observed (Fig. 8D, arrowhead), and the ependymal surface of the cerebellum is increased (asterisks in Fig. 8B,D), resembling the avian organization (compare Fig. 8D and Fig. 4A). Therefore, the extension of the ventricular surface of the velum at the expense of the vermis requires En1 function, while a moderate decrease in the size of the vermis is compatible with midline fusion.

We next contrasted *swaying* mutants (*Wnt1*$^{sw/sw}$, a natural mutant allele of *Wnt1*) (Thomas et al., 1991) with *En1*$^{+/Otx2lacZ}$ mutants (Broccoli et al., 1999). The least affected *swaying* mutants survive to adulthood and have two almost normally sized and well-organized cerebellar halves that do not fuse on the midline (Bronson and Higgins, 1991). In adult *En1*$^{+/Otx2lacZ}$ mutants, the cerebellar cortex is bisected by a midline sagittal

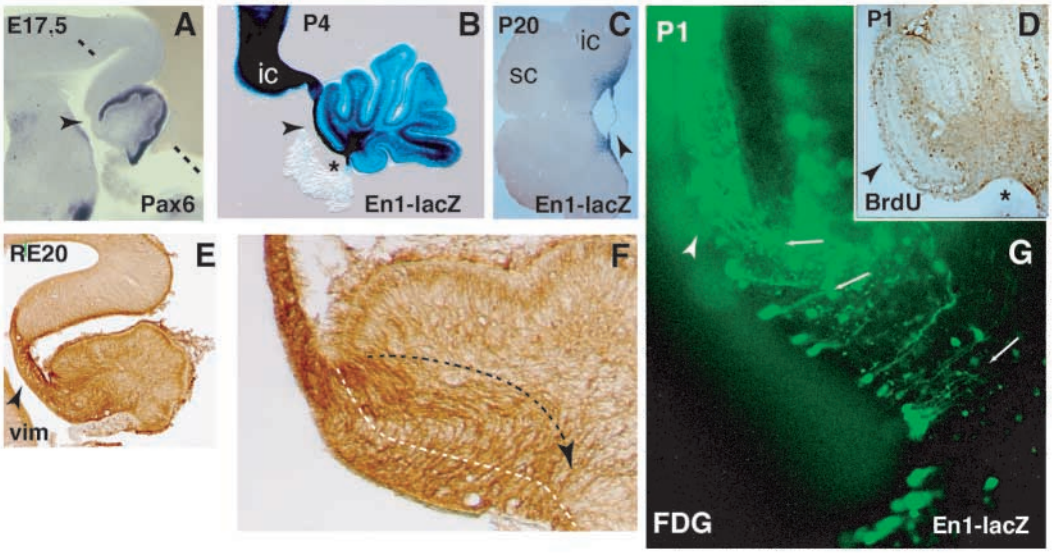


**Fig. 6.** Development of the velum medullaris in the mouse. (A,B,D-G) Sagittal and (C) horizontal sections through the MHB junction of mice (A-D,G) or rat (E,F). (A-G) The developmental age (top left) and marker used (bottom) are indicated on each image. (A) In late embryos, the Pax6-labeled EGL reaches the midbrain boundary; the velum medullaris (arrowhead) is very short at this stage. It develops during the following days and expresses high levels of En1, detected in B and C by X-gal staining of $En1^{Lki/+}$ mice Asterisk in B and D indicate cerebellar midline ependyme. The plane of section in C is indicated by the dashed line in A. (D) The high number of cells that incorporate BrdU in the velum compared to the ependymal surface of the cerebellum indicates that velum growth depends on active proliferation. (E,F) A specific set of radial glia cells labeled for vimentin (vim) link the velum (arrowhead in E) and the cerebellum ependyma. (F) Higher magnification of E. Black dashed line indicates the direction of cerebellar cortex retraction; white dashed line outlines the future extent of the velum medullaris. (G) These glia are outlined by the diffusible fluorescent β-galactosidase substrate FDG (arrow) in $En1^{Lki/+}$ pups indicating that they express high levels of En1. The arrowheads point to the velum medullaris. ic: inferior colliculus, sc: superior colliculus.

fissure (Broccoli et al., 1999). At first sight, except for the medial fiber bundle observed only in $En1^{+/Otx2lacZ}$, the adult cerebellar phenotypes of the $En1^{+/Otx2lacZ}$ and the least affected $Wnt1^{sw/sw}$ mutants seemed very similar (Fig. 8E-G). Upon inspection however, it became clear that with respect to the growth of the velum medullaris, they have opposite phenotypes. In $Wnt1^{sw/sw}$, the anterior cerebellum is fused to the inferior colliculus (Fig. 8I) and even intermixes with it (Bally-Cuif et al., 1995), and no intervening structure can be detected. On the midline, the cerebellar primordia of $Wnt1^{sw/sw}$ mutants are separated by a rostral extension of the choroid plexus (Fig. 8K). In $En1^{+/Otx2lacZ}$ animals, a wide sheet of cells forms a midline fold (Fig. 8H,J) between the two cerebellar halves. On the basis of its structure, this sheet of cells resembles much more the velum medullaris than the inferior colliculus. The Wnt1 expression domain, which is interrupted on the cerebellar midline of wild- type embryos, is continuous in $Wnt1^{sw/sw}$ mutants, suggesting that this specific domain of the rhombic lip does not develop in the mutants (Fig. 8O). In $En1^{+/Otx2lacZ}$ embryos, the two cerebellar primordia are widely separated by a medial domain (asterisk in Fig. 8K,L) expressing midbrain markers (Otx2 and ephrin A5) (Broccoli et al., 1999) and abut the choroid plexus (Fig. 8K). An interruption in the expression of roof plate markers (Wnt1; Fig. 8M,N) and a lack of convergence of rhombic lip markers (Math1; Fig. 8L) indicate that the continuity between the midbrain and hindbrain roof plates is lost in $En1^{+/Otx2lacZ}$ embryos. The transformation of a 'midbrain' territory intervening between the cerebellar primordia in $En1^{+/Otx2lacZ}$ embryos into a velum-like structure at later stages was not expected and is not fully understood (see Discussion). Nevertheless, this observation stresses that both lack and overgrowth of isthmic midline-derived structures – in particular the velum medullaris – interfere with midline cerebellar fusion. A schematic interpretation of the observed phenotypes is shown in Fig. 8P.

## Discussion

### Cell movements at the mid/hindbrain junction

We have identified a restricted dorsal midline domain at the MHB junction from which divergent streams of cells emigrate to populate the midbrain and cerebellar midlines. Previous fate map studies had uncovered complex morphogenetic movements at the MHB junction (Alvarez Otero et al., 1993; Millet et al., 1996). In particular, anteriorly directed movements were observed to originate only from the dorsomedial region close to the caudal limit of Otx2 expression (Millet et al., 1996). We find here that an adjacent, slightly more caudal group of cells produces the cerebellar midline (see also Alexandre and Wassef, 2003). Strip (type 4) graft experiments indicate that the lateral midbrain neuroepithelium converges medially. An apparent convergence could result from the mediolateral differences in caudal midbrain growth we observed. Since no preferential extension of the midline region was noticed in these grafts, it is unlikely that the divergent migration of midline cells is a direct consequence of global convergence-extension movements. Importantly for the process of cerebellar fusion, the overgrowing midbrain neuroepithelium must be

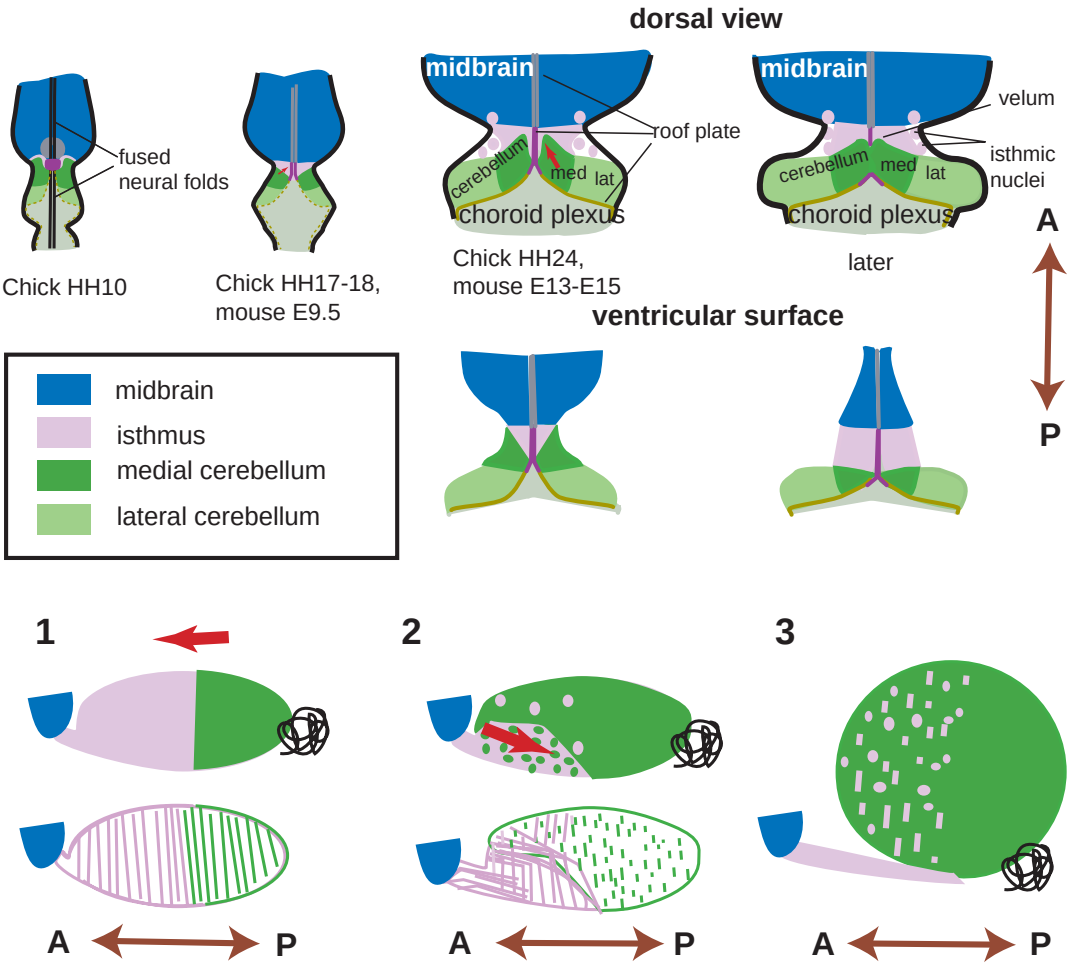


**Fig. 7.** Morphogenetic movements in the dorsal neural tube at the MHB junction, based on observations in chick and mouse. Midbrain-derived cells, blue; isthmus-derived, pink; cerebellum, green (darker for the vermis). Double-headed arrows indicate AP orientation. (Top) The two drawings on the left depict the formation of the cerebellum (purple) and caudal midbrain (gray) roof plate structures derived from a restricted midline region in chick HH10. The cerebellum then fuses (third drawing, chick HH24 and mouse E15) over an isthmus-derived territory. The fourth drawing illustrates the medial retraction of the cerebellar cortex in perinatal mice and the growth of the velum medullaris. Pink circles represent isthmic nuclei. The white area derives from the hindbrain. (Bottom) Seesaw motion of the cerebellar cortex over the isthmic-derived territory. Schematic sagittal sections through the isthmo-cerebellar region close to the midline. The choroid plexus (black coil) marks the posterior pole of the region. Red arrows indicate the direction of cerebellar cortex displacement. Global tissue displacements are illustrated in the upper panels 1 and 2, and in 3. The orientation of radial glia (thin pink and green lines) in the same sections is illustrated in the lower panels 1 and 2. In 2, the radial glia become bent by the sliding cerebellum; pink dots in 2 and 3 represent isthmus-derived interneurons.

constrained to the anterior. One of the functions of the MHB organizer, attested by the formation of the isthmic constriction or, upon induction of an organizer by FGF8 bead insertion, by the formation of an ectopic constriction (Martinez et al., 1999), is to maintain a tension at the MHB junction, which, in turn, prevents a global inversion of dorsal midbrain movements. Strikingly, this is precisely the case in E12.5 *En1*$^{+/Otx2lacZ}$ mutants, in which the caudal limit of Otx2 is shifted posteriorly and where, from E11.5 onward, the hindbrain appears widened (this study). In contrast, gene expression is minimally affected at early stages, mostly at the dorsal midline of the MHB (Broccoli et al., 1999), although the Otx2 limit is thought to position the organizer. The early morphogenetic defect is partially rescued in adult *En1*$^{+/Otx2lacZ}$ mutants (Broccoli et al., 1999). First, most of the domain of ectopic Otx2 expression develops as a velum medullaris; second, as the cerebellum grows postnatally, it becomes constrained laterally by the skull and forces the ectopic midbrain and velum structures anteriorly and medially, thus restoring the transverse orientation of the MHB limit.

## Formation of the hindbrain roof plate

The roof plate is a signaling center involved in dorsoventral patterning. In the spinal cord, the roof plate arises at the site of neural fold fusion under the influence of TGFβ family signals derived from the adjacent surface ectoderm (Liem et al., 1995). In the hindbrain, the dorsal part of the neural tube loses its epithelial organization and forms a sheet of cells on which the choroid plexus organizes. Roof plate structures form at the boundary between the choroid plexus and the dorsal edges of the neural epithelium, possibly under the influence of choroid plexus-derived BMP signals (Alder et al., 1999). At

the 12ss, the presumptive choroid plexus territory extends in rhombomere 1 (Gilthorpe et al., 2002) up to the isthmic constriction (this study). Cerebellar midline cells migrating from the isthmic region could prevent the rostral extension of the choroid plexus either by being refractory to a choroid plexus fate, or by propagating inhibitory signals. BMP signaling is essential for choroid plexus development, at least in the forebrain (Furuta et al., 1997; Hébert et al., 2002; Panchision et al., 2001), while BMP expression is downregulated on the cerebellar midline where Drm, a potent

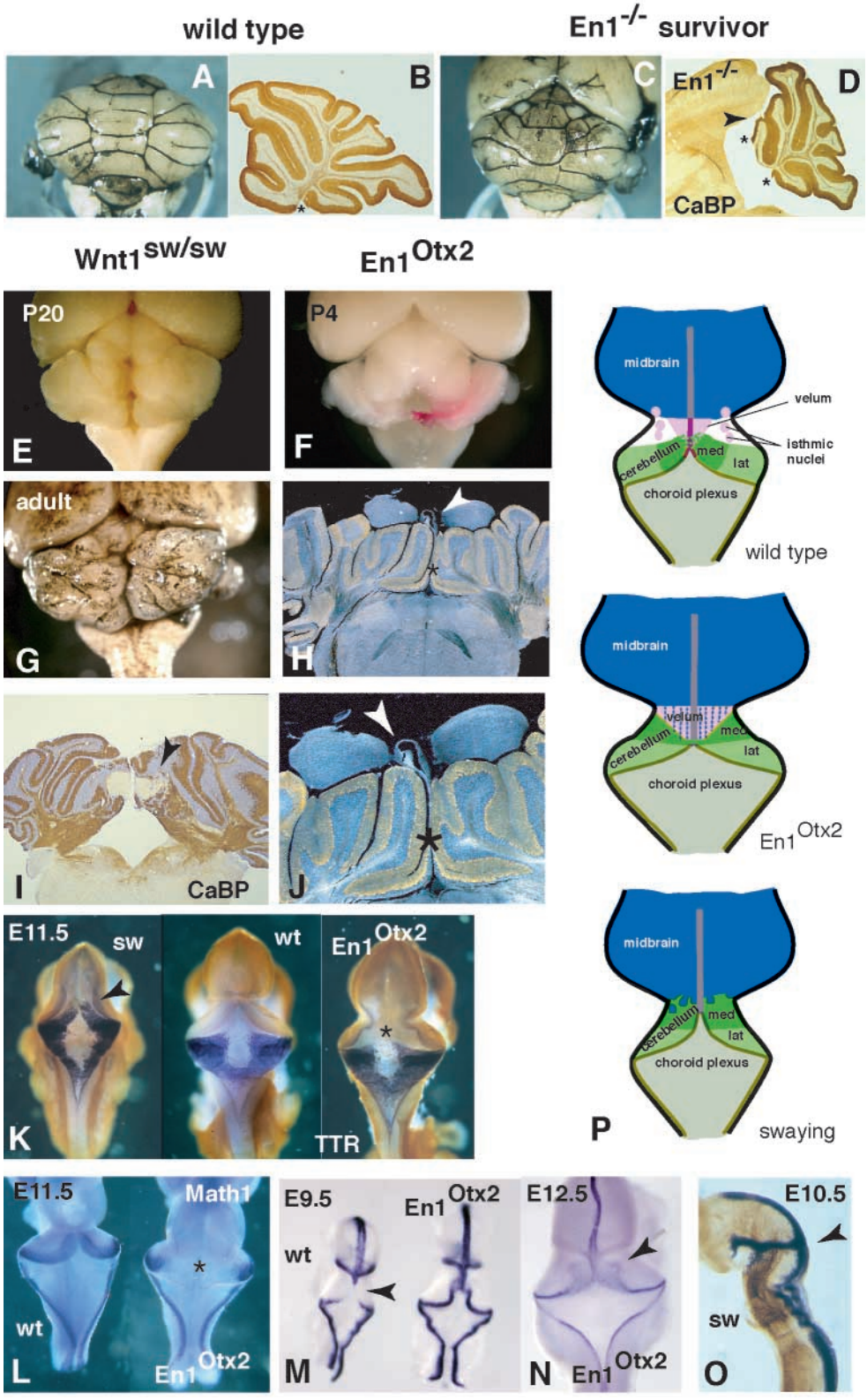


**Fig. 8.** Mid/hindbrain mutations interfere with cerebellar midline fusion. Whole-mount view (A,C) and midsagittal sections (B, D) through the cerebellum of adult wild-type (A,B) and *En1*$^{hd/hd}$ survivor mutants (C,D). Compared to wild type, the velum medullaris is shortened in adult *En1*$^{hd/hd}$ mutant survivors (arrowhead in D), and the ependymal surface of the cerebellum is widened (asterisks in B and D) indicating that En1 function is required for the partitioning of the ependymal surface between the velum and the vermis. (E-G) The postnatal cerebellum of *Wnt1*$^{sw/sw}$ at P20 (E) and *En1*$^{+/Otx2lacZ}$ at P4 (F) has a distinct gap on the midline that is reduced to a fissure in *Wnt1*$^{sw/sw}$ adults (G). (H,J) In adult *En1*$^{+/Otx2lacZ}$ mutants, the two cerebellar halves are separated by a wide sheet of cells that loops above the surface of the cerebellum (arrowheads). (I) In *Wnt1*$^{sw/sw}$, the anterior cerebellum is fused to the inferior colliculus (arrowhead). (K) Posterior views of E11.5 embryos where the choroid plexus has been labeled by Ttr in situ hybridization. Compared to wild type (wt) and *En1*$^{+/Otx2lacZ}$ (*En1*$^{Otx2}$) mutant embryos, the choroid plexus in *Wnt1*$^{sw/sw}$ (sw, arrowhead) extends anteriorly separating the cerebellar halves. (L-N) Modification of the cerebellar midline domain in *En1*$^{+/Otx2lacZ}$ mutants. (L) Math1 expression is interrupted on the midline in E11.5 embryos. (M,N) Wnt1 expression on the roof plate is prolonged in the hindbrain at E9.5 (compare with wild type; arrowhead, M). This expression becomes wider and fuzzy at later stages (E12.5, N). (O) In *Wnt1*$^{sw/sw}$ (sw) mutants at E10.5, Wnt1 expression (purple) is not interrupted in the cerebellar plate as observed in wild type. Axons are labeled in brown by neurofilament immunocytochemistry. (P) Schematic interpretation of the midline phenotypes of *Wnt1*$^{sw/sw}$ and *En1*$^{+/Otx2lacZ}$ mutants compared to wild type. Same color code as in Fig. 7.

BMP antagonist, is specifically expressed at the onset of choroid plexus development (Pearce et al., 1999).

### Transient expression of Math1 on the cerebellar midline

At early stages the two cerebellar primordia are delineated by a Math1-expressing rhombic lip. Consistent with earlier findings (Hallonet et al., 1990; Martinez and Alvarado-Mallart, 1989), we observed that the caudal midbrain strip grafts populate the cerebellar midline but do not produce GCs. The requirements for GC production are not met on the cerebellar midline: first, the rhombic lip to GCP switch requires BMP signals (Alder et al., 1999), which we find markedly decreased on the cerebellar midline and second, Math1, whose function is essential for GCP development (Ben-Arie et al., 1997) is also downregulated on the cerebellar midline. Slit2 has been shown to repel GCP (Gilthorpe et al., 2002). Slit1 and 2, expressed elsewhere in the rhombic lip, are also downregulated on the cerebellar midline (this study and unpublished observations), an event that could trigger cerebellar fusion, by first allowing GCP to populate the midline and then attracting PCs, known to migrate beneath ectopic patches of GCP in *Unc5h3* mutants (Ackerman et al., 1997; Leonardo et al., 1997; Przyborski et al., 1998). Finally, although the cerebellar midline is not favorable for the acquisition of roof plate or rhombic lip identities, several observations indicate that choroid plexus-derived signals, in particular BMPs, are capable of inducing or maintaining rhombic lip markers (Alder et al., 1999; Bally-Cuif et al., 1995; Furuta et al., 1997). The transient presence of a putative source of GCs in the midvermis could explain the previously puzzling observation that, whereas in situ the vermis primordium does not produce GCs (Hallonet et al., 1990; Martinez and Alvarado-Mallart, 1989) (present study), the ectopic structures with anterior cerebellum identity induced by FGF8 bead implantation have a normal complement of GCs (Martinez et al., 1999).

### Involvement of the dorsal isthmus in cerebellar morphogenesis

The observations reported here indicate that migration from the isthmic region provides the cerebellar midline with both a substratum and signals essential for cerebellar fusion. In rodent, an En1-dependent caudal retraction of the fused rostral cerebellar cortex is subsequently observed, partially reversing the cell movements leading to cerebellar fusion (see Fig. 7). Isthmus-derived cerebellar midline cells could be specialized in the production of GABAergic interneurons both in chick and mouse. However, the isthmus cannot be the sole source of this cerebellar cell type, as GABAergic interneurons are still present in the cerebellum of *Wnt1*$^{sw/sw}$ mutant mice that lack isthmic structures (unpublished observation).

The cerebellar phenotype of adult *Wnt1*$^{sw/sw}$ mutants, fusion of the cerebellum with the midbrain, deletion of intervening structures and anterior displacement of the choroid plexus, is consistent with our previous reports on *swaying* embryos (Bally-Cuif et al., 1995; Louvi and Wassef, 2000). In contrast, the increase in isthmic structures (generally considered as intermediate between rhombomere 1 and the midbrain) that we observed in the *En1*$^{+/Otx2lacZ}$ mutants was unexpected. Indeed, the shift in the caudal limit of Otx2 expression in *En1*$^{+/Otx2lacZ}$ mutants has been interpreted as an expansion of the midbrain territory at the expense of the anterior vermis (Broccoli et al., 1999). According to this scenario, any intervening isthmic territory should have been at best reduced, if not deleted. The present finding suggests that the isthmic territory is really an intermediate domain depending on both Otx2 and Gbx2. Delineation of the isthmic domain could occur at an early stage where the Otx2 and Gbx2 domains overlap (Garda et al., 2001). Alternatively, the isthmic domain could be composed of cells that cross the Otx2 caudal limit and switch off Otx2 expression. Although the caudal limit of Otx2 expression has been considered as fixed (Millet et al., 1996), several observations challenge this notion. Cells have been shown to cross the Otx2 boundary (Jungbluth et al., 2001), no restriction to cell coupling, a hallmark of rhombomere boundaries, has been found at the MHB junction (Martinez et al., 1992), and extensive DiI tracing experiments never detected any restriction to cell movements at the MHB junction except on the midline (Alexandre and Wassef, 2003). Finally the mode of progressive differentiation and growth of both the mid- and hindbrain centered at the MHB allows for much regulation when gene expression is turned off and on (Millet et al., 1999). We propose that maintenance of a moderate level of Otx2 expression in the hindbrain predisposes boundary cells towards an isthmic identity.

The observations reported here indicate that the isthmic region is crucial for the formation of the cerebellar midline, first, by controlling divergent midline cell movements and by contributing cells to both the cerebellar roof plate and the adjacent domain, second, by endowing the isthmus-derived cells in the cerebellar plate with specific properties and allowing them to restrict the influence of the choroid plexus, a hindbrain-specific midline cell population.

We thank C. Ragsdale and F. Bourrat for critical reading of successive versions of the manuscript, Rosette Goiame for technical help, A. Eichmann, B. Hamilton, A. Chédotal, F. Guillemot, B. Hogan, M. Marx, C. Ragsdale, M. Tessier-Lavigne and A. Tobin for providing plasmids for in situ probes, or antibodies. The QCPN and 2H3 monoclonal antibody were obtained from the Developmental Studies Hybridoma Bank. This work was supported by an EC Biotech grant to M.W. and W.W., an ACI Développement grant to M.W., and a FCT fellowship to P.A.

## References

**Ackerman, S. L., Kozak, L. P., Przyborski, S. A., Rund, L. A., Boyer, B. B. and Knowles, B. B.** (1997). The mouse rostral cerebellar malformation gene encodes an UNC-5-like protein. *Nature* **386**, 838-842.

**Alcántara, S., Ruiz, M., de Castro, F., Soriano, E. and Sotelo, C.** (2000). Netrin 1 acts as an attractive or as a repulsive cue for distinct migrating neurons during the development of the cerebellar system. *Development* **127**, 1359-1372.

**Alder, J., Lee, K. J., Jessell, T. M. and Hatten, M. E. (**1999). Generation of cerebellar granule neurons in vivo by transplantation of BMP-treated neural progenitor cells. *Nat. Neurosci.* **2**, 535-540.

**Alexandre, P. and Wassef, M.** (2003). The isthmic organizer links anteroposterior and dorsoventral patterning in the mid/hindbrain. *Development* **130**, 5331-5338.

**Altman, J. and Bayer, S. A.** (1985a). Embryonic development of the rat cerebellum. III. Regional differences in the time of origin, migration, and settling of Purkinje cells. *J. Comp. Neurol.* **231**, 42-65.

**Altman, J. and Bayer, S. A.** (1985b). Embryonic development of the rat cerebellum. I. Delineation of the cerebellar primordium and early cell movements. *J. Comp. Neurol.* **231**, 1-26.

**Alvarez Otero, R., Sotelo, C. and Alvarado-Mallart, R. M.** (1993). Chick/quail chimeras with partial cerebellar grafts: an analysis of the origin and migration of cerebellar cells. *J. Comp. Neurol.* **333**, 597-615.

**Andersson, G. and Oscarsson, O.** (1978). Climbing fiber microzones in cerebellar vermis and their projection to different groups of cells in the lateral vestibular nucleus. *Exp. Brain Res.* **32**, 565-579.

**Bally-Cuif, L. and Wassef, M.** (1994). Ectopic induction and reorganization of Wnt-1 expression in quail/chick chimeras. *Development* **120**, 3379-3394.

**Bally-Cuif, L., Cholley, B. and Wassef, M.** (1995). Involvement of Wnt-1 in the formation of the mes/metencephalic boundary. *Mech. Dev.* **53**, 23-34.

**Ben-Arie, N., Bellen, H. J., Armstrong, D. L., McCall, A. E., Gordadze, P. R., Guo, Q., Matzuk, M. M. and Zoghbi, H. Y.** (1997). Math1 is essential for genesis of cerebellar granule neurons. *Nature* **390**, 169-172.

**Ben-Arie, N., Hassan, B. A., Bermingham, N. A., Malicki, D. M., Armstrong, D., Matzuk, M., Bellen, H. J. and Zoghbi, H. Y. (**2000). Functional conservation of atonal and Math1 in the CNS and PNS. *Development* **127**, 1039-1048**.**

**Broccoli, V., Boncinelli, E. and Wurst, W.** (1999). The caudal limit of Otx2 expression positions the isthmic organizer. *Nature* **401**, 164-168.

**Bronson, R. T. and Higgins, D. C.** (1991). The swaying (sw) mutation causes a midline sagittal cerebellar fissure. *Mouse Genome* **89**, 851.

**Favor, J., Sandulache, R., Neuhauser-Klaus, A., Pretsch, W., Chatterjee, B., Senft, E., Wurst, W., Blanquet, V., Grimes, P., Sporle, R. and Schughart, K.** (1996). The mouse Pax2(1Neu) mutation is identical to a human PAX2 mutation in a family with renal-coloboma syndrome and results in developmental defects of the brain, ear, eye, and kidney. *Proc. Natl. Acad. Sci. USA* **93**, 13870-13875.

**Furuta, Y., Piston, D. W. and Hogan, B. L.** (1997). Bone morphogenetic proteins (BMPs) as regulators of dorsal forebrain development. *Development* **124**, 2203-2212.

**Garda, A. L., Echevarria, D. and Martinez, S.** (2001). Neuroepithelial co-expression of Gbx2 and Otx2 precedes Fgf8 expression in the isthmic organizer. *Mech. Dev.* **101**, 111-118.

**Gilthorpe, J. D., Papantoniou, E. K., Chedotal, A., Lumsden, A. and Wingate, R. J.** (2002). The migration of cerebellar rhombic lip derivatives. *Development* **129**, 4719-4728.

**Hallonet, M. E., Teillet, M. A. and Le Douarin, N. M.** (1990). A new approach to the development of the cerebellum provided by the quail-chick marker system. *Development* **108**, 19-31.

**Hallonet, M. E. and Le Douarin, N. M.** (1993). Tracing neuroepithelial cells of the mesencephalic and metencephalic alar plates during cerebellar ontogeny in quail-chick chimaeras. *Eur. J. Neurosci.* **5**, 1145-1155.

**Hamburger, V. and Hamilton, H. L. (**1951). A series of normal stages in the development of the chick embryo. *J. Morph.* **88**, 49-92.

**Hamilton, B. A., Frankel, W. N., Kerrebrock, A. W., Hawkins, T. L., FitzHugh, W., Kusumi, K., Russell, L. B., Mueller, K. L., van Berkel, V., Birren, B. W. et al.** (1996). Disruption of the nuclear hormone receptor RORalpha in staggerer mice. *Nature* **379**, 736-739.

**Hanks, M., Wurst, W., Anson-Cartwright, L., Auerbach, A. B. and Joyner, A. L.** (1995). Rescue of the En-1 mutant phenotype by replacement of En-1 with En-2. *Science* **269**, 679-682.

**Hawkes, R. and Eisenman, L. M. (**1997). Stripes and zones: the origins of regionalization of the adult cerebellum. *Perspect. Dev. Neurobiol.* **5**, 95-105.

**Hébert, J. M., Mishina, Y. and McConnell, S. K.** (2002). BMP signaling is required locally to pattern the dorsal telencephalic midline. *Neuron* **35**, 1029-1041.

**Herrup, K., Wetts, R. and Diglio, T. J.** (1984). Cell lineage relationships in the development of the mammalian CNS. II. Bilateral independence of CNS clones. *J. Neurogenet.* **1**, 275-288.

**Herrup, K. and Kuemerle, B.** (1997). The compartmentalization of the cerebellum. *Annu. Rev. Neurosci.* **20**, 61-90.

**Jungbluth, S., Larsen, C., Wizenmann, A. and Lumsden, A.** (2001). Cell mixing between the embryonic midbrain and hindbrain. *Curr. Biol.* **11**, 204-207.

**Lane, P. W.** (1967). *Mouse Newslett.* **36**, 40.

**Lawson, A., Schoenwolf, G. C., England, M. A., Addai, F. K. and Ahima, R. S.** (1999). Programmed cell death and the morphogenesis of the hindbrain roof plate in the chick embryo. *Anat. Embryol.* **200**, 509-519.

**Le Douarin, N.** (1969). Details of the interphase nucleus in Japanese quail (Coturnix coturnix japonica). *Bull. Biol. Fr. Belg.* **103**, 435-452.

**Leonardo, E. D., Hinck, L., Masu, M., Keino-Masu, K., Ackerman, S. L. and Tessier-Lavigne, M.** (1997). Vertebrate homologues of C. elegans UNC-5 are candidate netrin receptors. *Nature* **386**, 833-838.

**Li, J. Y., Lao, Z., and Joyner, A. L.** (2002). Changing requirements for Gbx2 in development of the cerebellum and maintenance of the mid/hindbrain organizer. *Neuron*. **36**, 31-43.

**Liem, K. F., Jr, Tremml, G., Roelink, H. and Jessell, T. M.** (1995). Dorsal differentiation of neural plate cells induced by BMP-mediated signals from epidermal ectoderm. *Cell* **82**, 969-979.

**Lin, J. C. and Cepko, C. L.** (1999). Biphasic dispersion of clones containing Purkinje cells and glia in the developing chick cerebellum. *Dev Biol.* **211**, 177-197.

**Liu, A. and Joyner, A. L. (**2001). Early anterior/posterior patterning of the midbrain and cerebellum. *Annu. Rev. Neurosci*. **24**, 869-896.

**Louvi, A. and Wassef, M.** (2000). Ectopic Engrailed 1 expression in the dorsal midline causes cell death, abnormal differentiation of circumventricular organs and errors in axonal pathfinding. *Development* **127**, 4061-4071.

**Lumsden, A., Sprawson, N. and Graham, A.** (1991). Segmental origin and migration of neural crest cells in the hindbrain region of the chick embryo. *Development* **113**, 1281-1291.

**Martinez, S. and Alvarado-Mallart, R. M.** (1989). Rostral cerebellum originates from the caudal portion of the so-called "mesencepahlic" vesicle: a study using chick/quail chimeras. *Eur. J. Neurosci.* **1**, 549-560.

**Martinez, S., Geijo, E., Sanchez-Vives, M. V., Puelles, L. and Gallego, R.** (1992). Reduced junctional permeability at interrhombomeric boundaries. *Development* **116**, 1069-1076.

**Martinez, S., Crossley, P. H., Cobos, I., Rubenstein, J. L. and Martin, G. R.** (1999). FGF8 induces formation of an ectopic isthmic organizer and isthmocerebellar development via a repressive effect on Otx2 expression. *Development* **126**, 1189-1200.

**Mathis, L., Bonnerot, C., Puelles, L. and Nicolas, J. F.** (1997). Retrospective clonal analysis of the cerebellum using genetic *laacZ*/*lacZ* mouse mosaics. *Development* **124**, 4089-4104.

**McMahon, A. P. and Bradley, A. (**1990). The Wnt-1 (int-1) proto-oncogene is required for development of a large region of the mouse brain. *Cell* **62**, 1073-1085.

**Millet, S., Bloch-Gallego, E., Simeone, A. and Alvarado-Mallart, R. M.** (1996). The caudal limit of *Otx2* gene expression as a marker of the midbrain/hindbrain boundary: a study using in situ hybridisation and chick/quail homotopic grafts. *Development* **122**, 3785-3797.

**Millet, S., Campbell, K., Epstein, D. J., Losos, K., Harris, E. and Joyner, A. L.** (1999). A role for Gbx2 in repression of Otx2 and positioning the mid/hindbrain organizer. *Nature* **401**, 161-164.

**Panchision, D. M., Pickel, J. M., Studer, L., Lee, S. H., Turner, P. A., Hazel, T. G. and McKay, R. D.** (2001). Sequential actions of BMP receptors control neural precursor cell production and fate. *Genes Dev.* **15**, 2094-2110.

**Pearce, J. J., Penny, G. and Rossant, J.** (1999). A mouse Cerberus/Dan-related gene family. *Dev. Biol.* **209**, 98-110.

**Przyborski, S. A., Knowles, B. B. and Ackerman, S. L.** (1998). Embryonic phenotype of Unc5h3 mutant mice suggests chemorepulsion during the formation of the rostral cerebellar boundary. *Development* **125**, 41-50.

**Shimamura, K., Hirano, S., McMahon, A. P. and Takeichi, M.** (1994). Wnt-1-dependent regulation of local E-cadherin and alpha N-catenin expression in the embryonic mouse brain. *Development* **120**, 2225-2234.

**Thomas, K. R. and Capecchi, M. R.** (1990). Targeted disruption of the murine int-1 proto-oncogene resulting in severe abnormalities in midbrain and cerebellar development. *Nature* **346**, 847-850.

**Thomas, K. R., Musci, T. S., Neumann, P. E. and Capecchi, M. R.** (1991). Swaying is a mutant allele of the proto-oncogene Wnt-1. *Cell* **67**, 969-976.

**Wingate, R. J. and Hatten, M. E.** (1999). The role of the rhombic lip in avian cerebellum development. *Development* **126**, 4395-4404.

**Wurst, W., Auerbach, A. B. and Joyner, A. L.** (1994). Multiple developmental defects in Engrailed-1 mutant mice: an early mid-hindbrain deletion and patterning defects in forelimbs and sternun. *Development* **120,** 2065-2075.

**Yuan, W., Zhou, L., Chen, J. H., Wu, J. Y., Rao, Y. and Ornitz, D. M.** (1999). The mouse Slit family: secreted ligands for ROBO expressed in patterns that suggest a role in morphogenesis and axon guidance. *Dev. Biol.* **212**, 290-306.